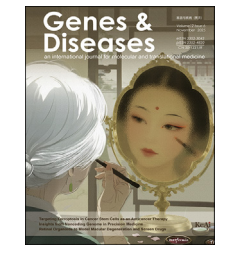


Available online at www.sciencedirect.com

# **ScienceDirect**



journal homepage: www.keaipublishing.com/en/journals/genes-diseases

RAPID COMMUNICATION

# Restored phagocytic ability of RPE patches derived from gene-corrected retinitis pigmentosa-hiPSCs on a biodegradable scaffold via clinical-grade protocol: Implications for autologous therapy



Cases of inherited retinal dystrophy (IRD) can be caused by mutations in the MERTK gene, which results in an autosomal recessive form of blindness (retinitis pigmentosa, RP) characterized by impaired phagocytosis of photoreceptor outer segments (POS) by retinal pigment epithelial cells (RPE). Persistent MERTK gene mutations in patient-derived human induced pluripotent stem cells (hiPSCs) pose a challenge for autologous stem cell-derived RPE replacement therapies targeting IRD. In a previous study, we created a hiPSC-based disease model of earlyonset RP caused by a mutation in the human MERTK gene (homozygous frameshift mutation c.992\_993del-CA(p.Ser331Cysfs\*5)).1 The hiPSC patient's derived RPE showed impaired POS phagocytosis. Applying CRISPR/Cas9 gene-editing technology supported the generation of heterozygously and homozygously corrected RP-hiPSC lines, RP1-FiPS4F1-GC1 and RP1-FiPS4F1-GC2, respectively. The RPE cells derived from these isogenic hiPSC recovered both wild-type MERTK protein expression and recovered the function of phagocytosis of POS.

We here expand the patient's RP-hiPSC, two genetically corrected hiPSC, and hiPSC derived from a healthy donor as control (Ctrl3-FiPS4F1) to a clinical-grade, triphasic monolayer differentiation protocol developed by Sharma et al<sup>3</sup> (resumed in Fig. S1A). This differentiation protocol induces the rapid generation of RPE clusters during the first differentiation phase compared with other spontaneous differentiation-based protocols.

Peer review under the responsibility of the Genes & Diseases Editorial Office, in alliance with the Association of Chinese Americans in Cancer Research (ACACR, Baltimore, MD, USA)

We observed an epithelial cell morphology of differentiating cells by day (D) 10, prompting a shift to the use of RPE Commitment Medium by D25 (Fig. S1B), which induced the spontaneous appearance of pigmented cell clusters in confluent neuroectodermal culture until D40 (Fig. S1B). At D40, we observed areas of cells with a polygonal, cobblestone-like morphology characteristic of mature RPE (Fig. S1B); therefore, we collected cells and isolated RPE by negative magnetic immunoreactivity (CD24<sup>-</sup> and CD56<sup>-</sup>) from a single cell suspension. The employed cell lines showed variable efficiency in RPE yield (from 20% to 50%, data not shown).

To translate our approach to the clinic, we recently described a scaffold consisting of a biodegradable ultrathin nanofibrous membrane made of poly(L-lactide-co-D, L-lactide) (PDLLA) and an embedded peripheral supporting oval frame optimized for RPE growth. 4 The CD24 -/ CD56 - hiPSCderived RPE cells (hiPSC-RPE) were seeded onto the PDLLA scaffolds (Fig. S1B) for eight weeks to allow their maturation and polarization. A similar hexagonal morphology and high level of pigmentation were acquired in all four genetic backgrounds (Fig. 1A; Fig. S1C). The gene expression for trait RPE markers (BEST1, CRALBP, and RPE65) was significantly higher compared with respective undifferentiated hiPSC lines (Fig. 1B). The absence of pluripotency-associated markers such as NANOG in all four hiPSC-RPE cell lines was observed (Fig. 1B). Ultrastructural studies using transmission electron microscopy confirmed the correct apical location of microvilli and lateral cell-cell junctions (tight junctions) of RPE-like patches derived from all four hiPSC lines (detailed representative transmission electron microscopy analysis presented in Fig. S2A) with all subcellular like intercellular junctional

2 Rapid Communication

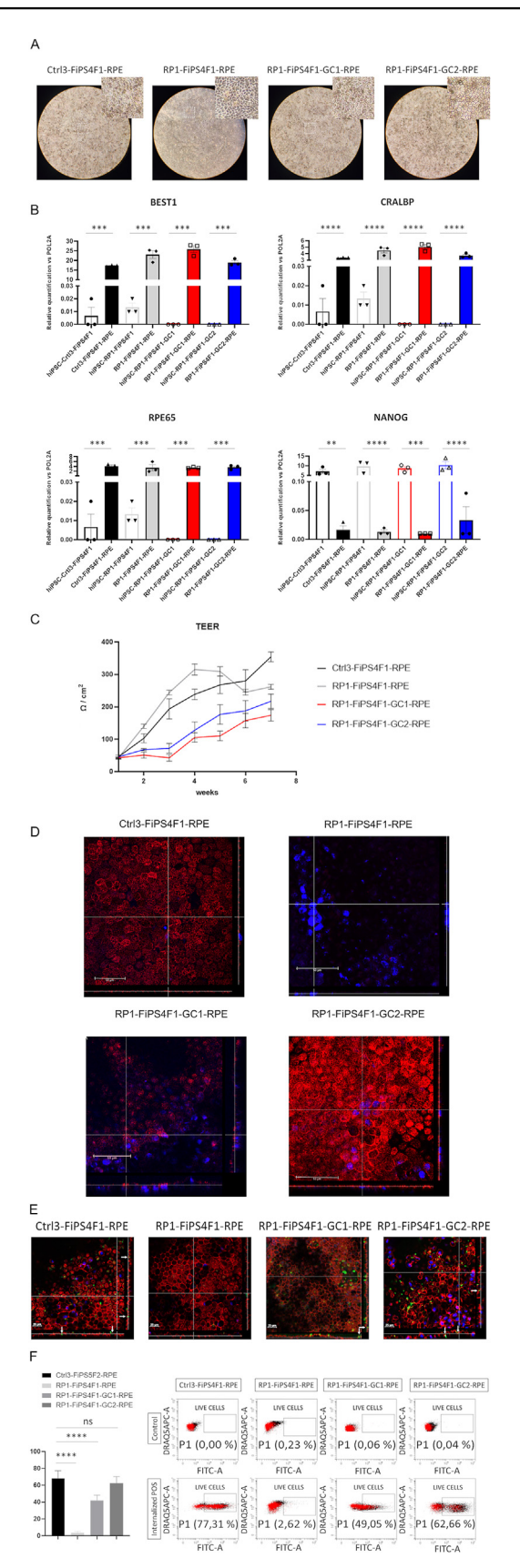


**Figure 1** Functional characterization of RPE derived from patient's, genetically corrected, and healthy hiPSC lines. **(A)** Representative pictures of the cells cultured in plastic dishes 7 days in parallel to inserts with higher magnification (digital

melanosomes (black round and oval shapes in Fig. S2A) displayed an apical distribution and basal infoldings on nanofibrous scaffolds (Fig. S2A). All other RPE cells acquired a similar cellular morphology (Fig. S2B).

The RPE maturity was validated by trans-epithelial electrical resistance (TEER) measurements made during the eight weeks of cell culture on nanofibrous membranes, and progressively increasing TEER values ( $150-400~\Omega/cm^2$ ) over time were demonstrated, suggesting the gradual maturation of RPE cells on PDLLA membranes (Fig. 1C).

To determine the reversion of the MERTK expression after mutation correction, we used an antibody that specifically detects the N-terminal fragment of MERTK. Immunofluorescence staining confirmed the expression of MERTK and its correct apical localization in RPE cells derived from gene-edited cell lines RP-hiPSCs and control hiPSCs while the original RP-hiPSCs lacked MERTK expression as reported in our previous study (Fig. 1D).

The immunocytochemical analysis revealed the expression of CRALBP, RPE65, BEST1, the microvilli marker EZRIN (proper localization), and the tight junction marker zonula occludens-1 (ZO-1) in RPE cells derived all four hiPSC lines (Fig. S3).

zoom-small micrograph). (B) RPE-associated gene expression in hiPSC-RPE. Quantitative reverse-transcription PCR analysis of mRNA expression for RPE markers (BEST1, CRALBP, and RPE65) and the pluripotency marker NANOG. Data represents the foldchange in mRNA expression of four RPEs relative to their parental hiPSCs. Each bar represents the mean  $\pm$  standard error of the mean (SEM) of six independent biological replicates (\*\* $p \le 0.01$ , \*\*\* $p \le 0.001$ , \*\*\*\* $p \le 0.0001$ ). (C) The barrier function of RPE cells grown in inserts was measured by transepithelial electrical resistance (TEER). Increasing TEER values were observed in RPE patches during differentiation. Each bar represents the mean  $\pm$  SEM of three independent biological replicates. (D) MERTK expression in RPE derived from hiPSCs analyzed by immunocytochemistry. Confocal z-stacks micrographs show apical MERTK distribution in RPE from gene-corrected (RP1-FiPS4F1-GC1 and RP1-FiPS4F1-GC2) and healthy control (Ctrl3-FiPS4F1) hiPSCs only. (E) In vitro phagocytosis assay of POS by RPE patches. Horizontal z-stacks together with vertical section simulation by Leica LAS software. RPE patches originating from control hiPSCs and gene-corrected RP-hiPSCs exhibited internalization of FITC-labeled POS (shown in green, indicated by arrows), and RP-hiPSCs-RPEs did not contain internalized POS. F-actin was stained by phalloidin (red) to visualize cell morphology. Images were taken with a Leica confocal microscope TCS SP8 using HCX PL APO lambda blue 63X/1.4 OIL objective. Scale bar, 10 μm. (F) Quantification of phagocytosis assay by flow cytometry. The graph represents the percentage of phagocytic RPE cells containing internalized POS (cells without incubation with POS-FITC). Healthy control, Ctrl3-FiPS4F1-RPEs. Each bar represents the mean  $\pm$  SEM of at least three independent biological replicates (\* $p \le 0.05$ , \*\* $p \le 0.01$ , \*\*\* $p \le 0.001$ , \*\*\*\* $p \le 0.0001$ ). The plots show the results of one representative experiment. Cells with internalized POS-FITC (phagocytes) are placed in the upper right quadrant (DRAQ5 and FITC-positive cells). RPE, retinal pigment epithelial cells; hiPSC, human induced pluripotent stem cell; RP, retinitis pigmentosa.

Rapid Communication 3

To assess the POS phagocytosis ability, we incubated the RPE cells with isolated bovine-derived fluorescently labeled POS¹ and monitored POS ingestion via confocal imaging. We observed that RPE patches generated from gene-corrected hiPSCs regained their ability to phagocytose POS unlike the original patient-derived RPE (Fig. 1E, arrows). In the case of patient-derived hiPSC, POS internalization was not observed, as only a few POS were found in the microvilli area outside of the cells.

The flow cytometry was employed to quantify the fraction of RPE with internalized POS (Fig. 1F). We observed a similar percentage of *POS*<sup>+</sup> RPE cells derived from genecorrected hiPSCs to both allele-corrected and control hiPSCs (67% and 71%, respectively, while the levels of phagocytosis in heterozygously corrected cells were lower (47%) compared with control healthy cells (Fig. 1F). As expected, significantly lower number of cells phagocytosing POS in mutation bearing hiPSC-RPE cells (4%) was observed compared with control (Fig. 1F).

As a novelty, our results support the user-independent nature of the differentiation protocol and its scalability to patient-derived and gene-corrected hiPSCs.<sup>3</sup> In addition, we reproduced methods for clinical-grade hiPSC subculture, cryopreservation, and differentiation to establish protocols for clinical applications. To our knowledge, this is the first study to describe the generation of RPE cells under clinical-grade protocol from genetically corrected hiPSC lines.

All RPE patches displayed multiple features of primary RPE; they grew as an epithelial monolayer with a cobblestone morphology, possessed apical pigmented melanosomes and basal nuclei, and expressed proteins involved in the process of retinol cycling upon culture on FDA-approved scaffolds. TEER measurements confirm a cell monolayer's overall health and confluence, with an increased value representing a strong barrier against an electric current, confirming native-RPE-like morphology and functionality.

We also confirmed the re-establishment of the expression of full-length MERTK protein and the complete reversion of lost phagocytic function of RPE patches derived from gene-corrected RP-hiPSCs. Gene correction of one or both alleles restored MERTK expression lost in the patient's cells. As suggested in our previous study,<sup>5</sup> only fully recovered protein would facilitate a functional improvement *in vivo*; overall, our current findings represent a clear step towards autologous therapy for MERTK-related HRD.

Our protocol significantly shortens differentiation times to about ten weeks, considering that RPE patches will be transplanted into the patients after four weeks of culture in inserts. This could allow us to reduce the time from the diagnosis to the implication of the treatment in patients with retinal diseases associated with RPE atrophy.

In this study, for the first time, the biodegradable, clinically approved nanofibrous scaffold is used to support differentiation towards RPE cell fate.<sup>4</sup> PDLLA membrane scaffolds compared to PLGA scaffolds slowly degrade after five months *in vitro*,<sup>4</sup> a timespan favorable for long-term RPE culture followed by mechanical handling during surgery<sup>4</sup> making it a better option for long-term support of transplanted cells. This innovation has critical implications for translational applications, as scaffold material is a key determinant of implant success.

To conclude, this study demonstrates a promising therapeutic option that combines hiPSC generation and differentiation, gene editing, and tissue engineering to create a potentially long-lasting autologous treatment for vision loss. The data generated from this study will be used as a foundation for the future evaluation of RPE patches in small and large animal preclinical models.

### CRediT authorship contribution statement

Rodriguez-Jimenez Francisco Javier: Writing - review & editing, Visualization, Methodology, Formal analysis, Data curation. Artero-Castro Ana: Writing — review & editing, Methodology, Investigation, Data curation. Studenovska Hana: Writing - review & editing, Methodology. Selles Francisca: Methodology, Investigation. Arteaga Claramunt Alba Maria: Investigation. Brymova Anna: Investigation. Jendelova Pavla: Writing — review & editing. Motlik Jan: Writing — review & editing, Funding acquisition. **Petrovski Goran:** Writing — review & editing. Lvtvvnchuk Lvubomvr: Writing — review & editing. Ardan Taras: Writing — review & editing. Tichotová Lucie: Validation. Drutovič Saskia: Validation. Sharma Ruchi: Writing - review & editing, Validation, Methodology. Lukovic Dunja: Writing — review & editing, Resources, Methodology. Bharti Kapil: Writing review & editing, Validation, Methodology. Erceg Slaven: Writing - review & editing, Writing - original draft, Visualization, Validation, Supervision, Resources, Project administration, Methodology, Investigation, **Funding** acquisition, Formal analysis, Data curation, Conceptualization.

## Data availability

No new data were generated or analyzed in support of this research.

### Conflict of interests

The authors declared no conflict of interests.

### **Funding**

The study was supported by the Norway Grants and Technology Agency of the Czech Republic (KAPPA project No. TO01000107), European Regional Development Fund by Programme Johannes Amos Comenius (No. CZ.02.01.01/00/ 22\_008/0004562 Project "Excellence in Regenerative Medicine"). Part of the equipment employed in this work has been funded by Generalitat Valenciana and co-financed with ERDF funds (OP ERDF of Comunitat Valenciana 2014-2020). This work was supported by funds from Foundation AFM-Telethon (21180) and Fundación Marató TV3 with Ref: 202010-10 and CIAICO/2021/115. This work also was supported by funds from Instituto de Salud Carlos III (ISCIII) of the Spanish Ministry of Health (PI20/01119 to D.L. co-funded by European Regional Development Fund [FEDER funds] "A Way to Make Europe") and Univerdidad CEU Cardenal Herrera grant GIR 23/04. The funding

4 Rapid Communication

organizations had no role in the design or conduct of this research.

### Appendix A. Supplementary data

Supplementary data to this article can be found online at https://doi.org/10.1016/j.gendis.2025.101609.

### References

- Lukovic D, Artero Castro A, Delgado AB, et al. Human iPSC derived disease model of MERTK-associated retinitis pigmentosa. Sci Rep. 2015;5:12910.
- Artero Castro A, Long K, Bassett A, et al. Generation of genecorrected human induced pluripotent stem cell lines derived from retinitis pigmentosa patient with Ser331Cysfs\*5 mutation in MERTK. Stem Cell Res. 2019;34:101341.
- Sharma R, Bose D, Montford J, Ortolan D, Bharti K. Triphasic developmentally guided protocol to generate retinal pigment epithelium from induced pluripotent stem cells. STAR Protoc. 2022;3(3):101582.
- Lytvynchuk L, Ebbert A, Studenovska H, et al. Subretinal implantation of human primary RPE cells cultured on nanofibrous membranes in minipigs. *Biomedicines*. 2022;10(3):669.
- Artero-Castro A, Long K, Bassett A, et al. Gene correction recovers phagocytosis in retinal pigment epithelium derived from retinitis pigmentosa-human-induced pluripotent stem cells. *Int* J Mol Sci. 2021;22(4):2092.

Rodriguez-Jimenez Francisco Javier <sup>a</sup>, Artero-Castro Ana <sup>a</sup>, Studenovska Hana <sup>c</sup>, Selles Francisca <sup>a</sup>, Arteaga Claramunt Alba Maria <sup>a</sup>, Brymova Anna <sup>d</sup>, Jendelova Pavla <sup>l</sup>, Motlik Jan <sup>d</sup>, Petrovski Goran <sup>e,f,g</sup>, Lytvynchuk Lyubomyr <sup>h,i</sup>, Ardan Taras <sup>d</sup>, Tichotová Lucie <sup>d</sup>, Drutovič Saskia <sup>d</sup>, Sharma Ruchi <sup>j</sup>, Lukovic Dunja <sup>k</sup>, Bharti Kapil <sup>j</sup>, Erceg Slaven <sup>a,b,\*</sup>

<sup>a</sup> Stem Cells Therapies in Neurodegenerative Diseases Lab, Centro de Investigación Principe Felipe (CIPF), Valencia 46012, Spain <sup>b</sup> National Stem Cell Bank-Valencia Node, Research Centre Principe Felipe, c/Eduardo Primo Yúfera 3, Valencia 46012, Spain

<sup>c</sup> Institute of Macromolecular Chemistry, Academy of Sciences of the Czech Republic, Prague 16206, Czech Republic

<sup>d</sup> Institute of Animal Physiology and Genetics, Academy of Sciences of the Czech Republic, Libechov 27721, Czech Republic

<sup>e</sup> Center for Eye Research and Innovative Diagnostics, Department of Ophthalmology, Institute for Clinical Medicine, Faculty of Medicine, University of Oslo, Oslo 0450, Norway

f Department of Ophthalmology, University of Split School of Medicine and University Hospital Centre, Split 21000,

<sup>g</sup> Department of Ophthalmology, Oslo University Hospital, Oslo 0450, Norway

<sup>h</sup> Department of Ophthalmology, Justus Liebig University Giessen, University Hospital Giessen and Marburg GmbH, Giessen 35392, Germany

<sup>1</sup> Karl Landsteiner Institute for Retinal Research and Imaging, Vienna 1030, Austria

<sup>3</sup> Ocular and Stem Cell Translational Research Section, National Eye Institute, NIH, Bethesda, MD 20892, USA <sup>k</sup> Department of Animal Production and Health, Public Veterinary Health and Food Science and Technology, School of Veterinary Medicine; Universidad Cardenal Herrera-CEU, CEU Universities, C/ Assegadors n° 2 Alfara del Patriarca, 46115 Valencia, Spain

<sup>1</sup>Institute of Experimental Medicine, Czech Academy of Sciences, Department of Neuroregeneration, Prague 14220, Czech Republic

\*Corresponding author. Stem Cells Therapies in Neurodegenerative Diseases Lab, Research Center "Principe Felipe", c/Eduardo Primo Yufera 3, Valencia 46012, Spain. *E-mail address*: serceg@cipf.es (E. Slaven) 22 March 2024

Available online 22 March 2025